Micro and Nano Systems Letters

CORRESPONDENCE

Open Access

Spray-printed ZnO thin film for high-sensitivity NO_2 gas sensing

Mohamed Ahmed Belal[1], Sugato Hajra[1], Swati Panda[1], Kushal Ruthvik Kaja[1], Kyeong Jun Park[1] and Hoe Joon Kim[1*]

Abstract

The controlling and precise detection of nitrogen dioxide (NO_2) gas is important in many industrial processes such as medical, petrochemical, and agriculture. Therefore, this study investigates the gas sensing performance of zinc oxide (ZnO) nanosheets prepared using a hydrothermal approach. The morphology and structure of the as-prepared material were analyzed using analysis techniques, including transmission electron microscope (TEM), scanning electron microscope (SEM), X-ray photoelectron spectroscopy (XPS), and X-ray diffraction (XRD). The ZnO ink was spray printed in a square design onto an oxidized silicon wafer substrate, which includes a lithographically designed interdigitated pattern. ZnO nanosheets exhibited superior gas sensing performance, which is 5298% for sensor response and 96 and 600 s for response and recovery times, respectively, at 150 °C and 100 ppm of NO_2 gas. The previous results emphasize applying the proposed spray printing technique in different applications because of straightforward, versatile for different substrates, and cost-effective.

Keywords NO_2 gas, Toxic gases, Spray printing, Lithography IDE, ZnO

*Correspondence:
Hoe Joon Kim
joonkim@dgist.ac.kr

Graphical Abstract

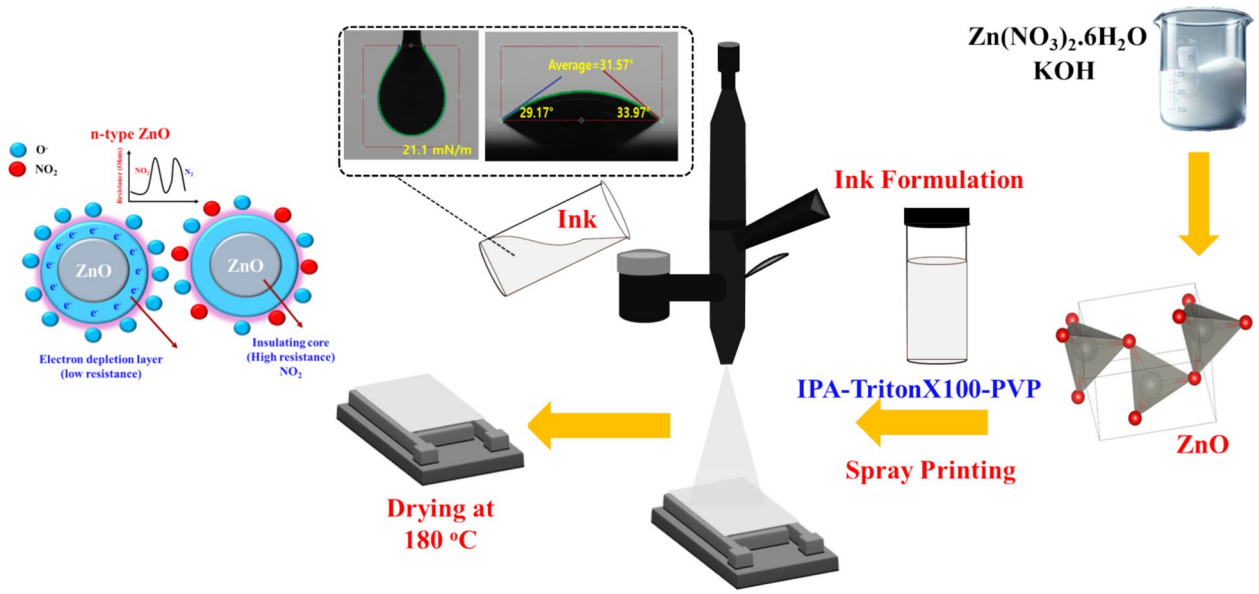

Introduction

Nitrogen dioxide (NO_2) is considered the most harmful gas, as emphasized by various published research articles and global organizations such as the American Conference of Governmental Industrial Hygienists (ACGIH), the American Lung Association (ALA), and the National Air Quality Monitoring Network (NAQMN) [1–8]. To illustrate, vehicle emissions, petrochemical industries, power plants, and the burning of fossil fuels are the sources of NO_2 gas, which is emitted to the outdoor environment. According to previous organizations, long-time exposure to NO_2 leads to health problems such as respiratory and cardiovascular diseases; moreover, it can contribute to environmental issues [4, 7, 9]. Therefore, the accurate detection and monitoring of NO_2 are critical for minimizing its harmful effects and ensuring compliance with environmental standards [6, 10–12].

The gas sensors with highly sensitive to NO_2 gas indoors or outdoors play a critical role in industrial safety and healthcare applications. Therefore, zinc oxide (ZnO) stands out among the materials used due to its high electron mobility, chemical stability, and strong affinity for gas molecules [3]. For fabrication, printing technologies have emerged as a promising approach for fabricating high-quality thin films, including those used in supercapacitors [13–15], and gas sensors [16–19], compared to vacuum filtration and drop casting. Moreover, the printing technologies are economical and scalable and can create uniform and smooth films on surfaces of different shapes and sizes. They provide precise control over the thickness and structure of the films, which is essential for enhancing sensor functionality. Additionally, spray printing, which is one of the printing technologies, can support the incorporation of a wide range of functional materials, fostering innovation in sensor technology [20–24].

Our present study focuses on the synthesis of ZnO nanosheets fabricated via a hydrothermal approach and testing it towards NO_2 gas. The as-prepared ZnO was morphologically and structurally analyzed using different techniques such as transmission electron microscope (TEM), scanning electron microscope (SEM), X-ray photoelectron spectroscopy (XPS), and X-ray diffraction (XRD). To evaluate the gas sensor performance, the fabricated ZnO sensor was tested under different temperatures of 25, 100, and 150 °C with different NO_2 concentrations of 20, 40, 60, 80, and 100 ppm to ensure the capability of the sensor to detect the gas. The sensor showed remarkable response, achieving a 5298% response with response and recovery times of 96 and 600 s, respectively, at 150 °C and 100 ppm NO_2. These findings highlight the potential of ZnO nanosheets as an effective NO_2 sensor, addressing critical needs in environmental monitoring by offering high performance and selectivity.

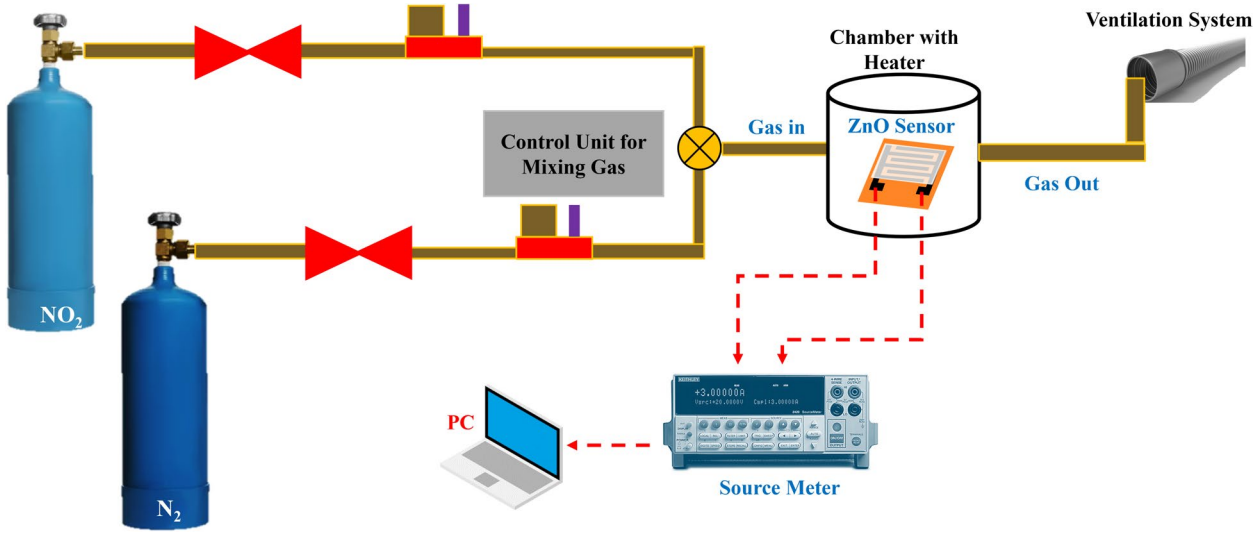

Fig. 1 Schematic diagram of the NO_2 gas sensing system

Table 1 Target NO_2 gas concentrations and adjusting of flow rate using the MFC

Target NO_2 gas concentration in NO_2/N_2 cylinder (ppm)	NO_2/N_2 (SCCM)	Pure N_2 (SCCM)	Total flow (SCCM)
100	100	0	100
80	80	20	100
60	60	40	100
40	40	60	100
20	20	80	100

Materials preparation

Materials

Thermo Scientific and Sigma-Aldrich, USA, supplied zinc nitrate hexahydrate ($Zn(NO_3)_2{\cdot}6H_2O$), polyvinylpyrrolidone (PVP, Mwt. 40000), and Triton X-100. Moreover, the PVP was used as a binder and stabilizer in the ink formulation, which utilized laboratory-grade isopropanol (IPA) sourced from Fisher Scientific, USA, as the main solvent.

Synthesizing of ZnO nanosheets and ink formulation

The synthesis of ZnO nanosheets started with the preparation of a solution containing 0.05 M $Zn(NO_2)_2{\cdot}6H_2O$ dissolved in 25 mL of deionized water (DI). To this solution, 0.8 M KOH was dissolved in 25 mL of DI and added dropwise under vigorous stirring for 1 h to ensure proper mixing. The resulting mixture was relocated into a 100 mL Teflon-lined autoclave and hydrothermally treated at 120 °C for 6 h. After synthesis, the ZnO nanosheets were washed three times through centrifugation to remove any residual materials. The washed nanosheets were then dried at 80 °C for 6 h to obtain the final product. To formulate the ZnO nanosheet ink, the nanosheets were dispersed at a concentration of 10 $mg{\cdot}mL^{-1}$ in IPA to optimize surface tension and wettability. PVP (2 $mg{\cdot}mL^{-1}$) and Triton X-100 (10 $\mu L{\cdot}mL^{-1}$) were added to ensure uniform distribution of the ZnO in IPA. The formulated ink was subjected to sonication for 60 min to enhance the dispersion and stability of the ZnO.

Experiments

Materials characterization

The synthesized ZnO nanosheets were subjected to full analysis utilizing various techniques to examine their morphology, structure, and composition. The XRD technique identified the crystal structure of the materials using the XRD, M/S Rigaku Mini Flex 600, Japan, which utilized Cu-K_α radiation with a wavelength (λ) of 1.5418 Å. We used a dual-source Thermo VG Escalab 250Xi to conduct XPS test of materials composition. The X-ray source was a monochromatic Al-K_α line, and the base pressure was 10^{-7} mbar. This allowed us to get a good look at the surface chemistry and elemental composition. The surface morphology and elemental mapping were investigated using TEM (JEOL JEM 2011) and SEM (model SU-8230, Japan), respectively, in conjunction with energy-dispersive X-ray spectroscopy (EDX) analysis from Oxford Instruments. The vacuum gas-sensing

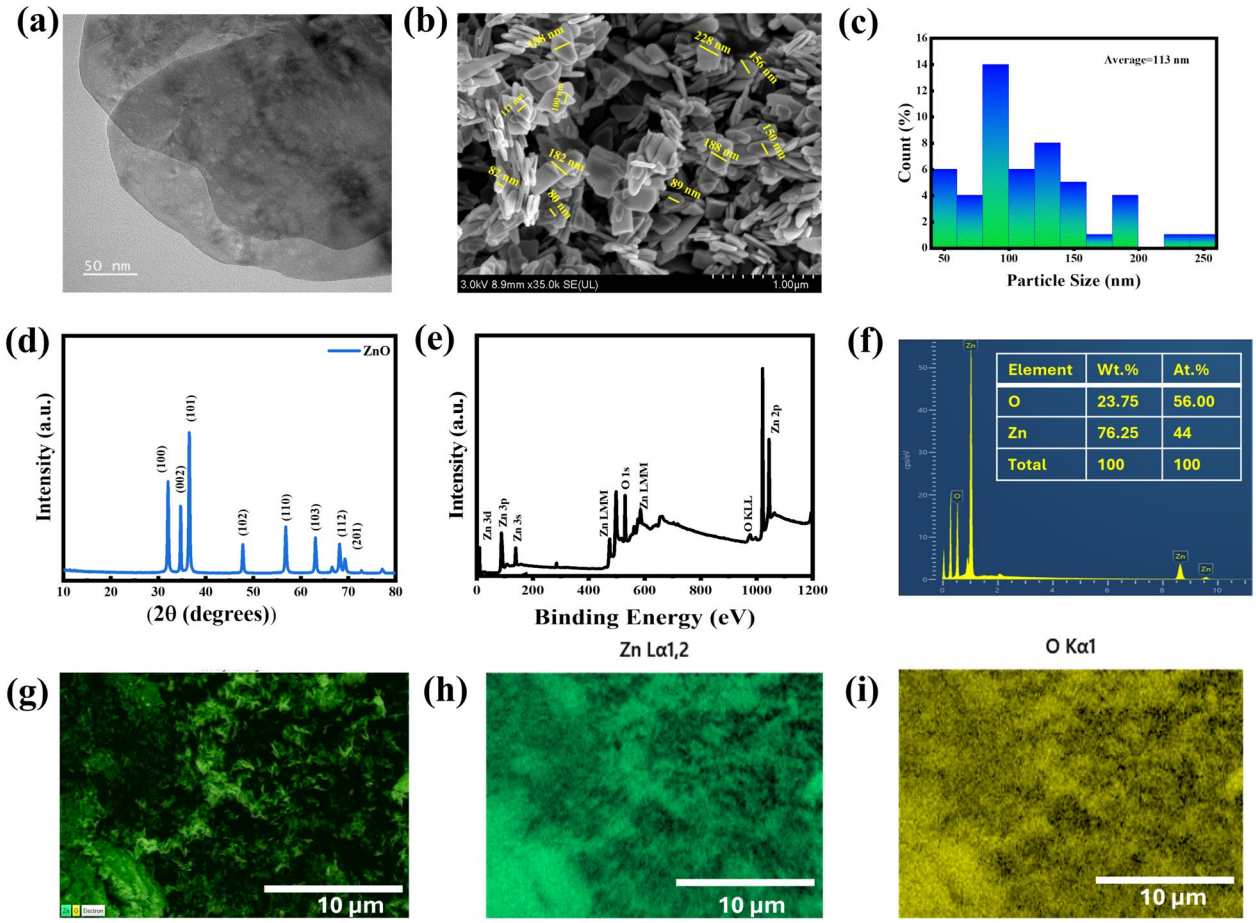

Fig. 2 Surface morphology and nanostructure characterizations of ZnO: **a** Transmission Electron Microscopy (TEM), **b** Scanning Electron Microscopy (SEM), **c** Particle size distribution (PSD), **d** X-ray Diffraction (XRD), **e** X-ray Photoelectron Spectroscopy (XPS) survey, and **f**–**i** SEM color mapping and atomic percentage (at%) of the ZnO

probe station manufactured by MS-TECH in Korea was used to conduct gas-sensing measurements on the ZnO gas sensor, which connected with a source meter (Keithley 2400c, USA).

Spray printing

The spray printing of ZnO ink over an interdigitated electrode (IDE) prepared by lithography technique over an oxidized silicon wafer is important to achieve consistent deposition and accurate control of the thickness. The ZnO was spray printed in a square pattern onto the IDE device of dimensions 4 mm in width and 5 mm in length with an area of 0.2 cm^2, using a solution containing 10 $mg{\cdot}mL^{-1}$ of ZnO. It was essential to maintain a distance of roughly 5 cm between the spray gun and the substrate to achieve a uniform film with a pressure of 20 PSI of the air compressor to control the thickness of the printed ZnO. The thickness of the printed material was precisely regulated by modifying the distance and the volume of ink dispensed from the nozzle, which was approximately 500 μL with a mass loading of around 5 mg in an area of 0.2 cm^2.

Gas sensing measurements

The gas sensing setup, depicted in Fig. 1, consisted of N_2 and NO_2/N_2 gas sources, with controlled concentrations of NO_2 flow to the gas chamber via mass flow controllers (MFCs) as seen in Table 1. The NO_2/N_2 gas mixture cylinder contains NO_2 at a concentration of 100 ppm, whereas the N_2 cylinder contains pure nitrogen. Within the chamber, the ZnO sensor was positioned on a block-shaped heater, and its temperature was regulated using a temperature controller module. The performance of the sensor was evaluated at the optimal operating temperatures of 25, 100, and 150 °C, with NO_2 concentrations ranging from 20 to 100 ppm. To assess the performance of the chemiresistive gas sensor, the baseline resistance (R_a) and the resistance in the presence of NO_2 gas (R_g) were measured at 80 V of bias. These measurements were

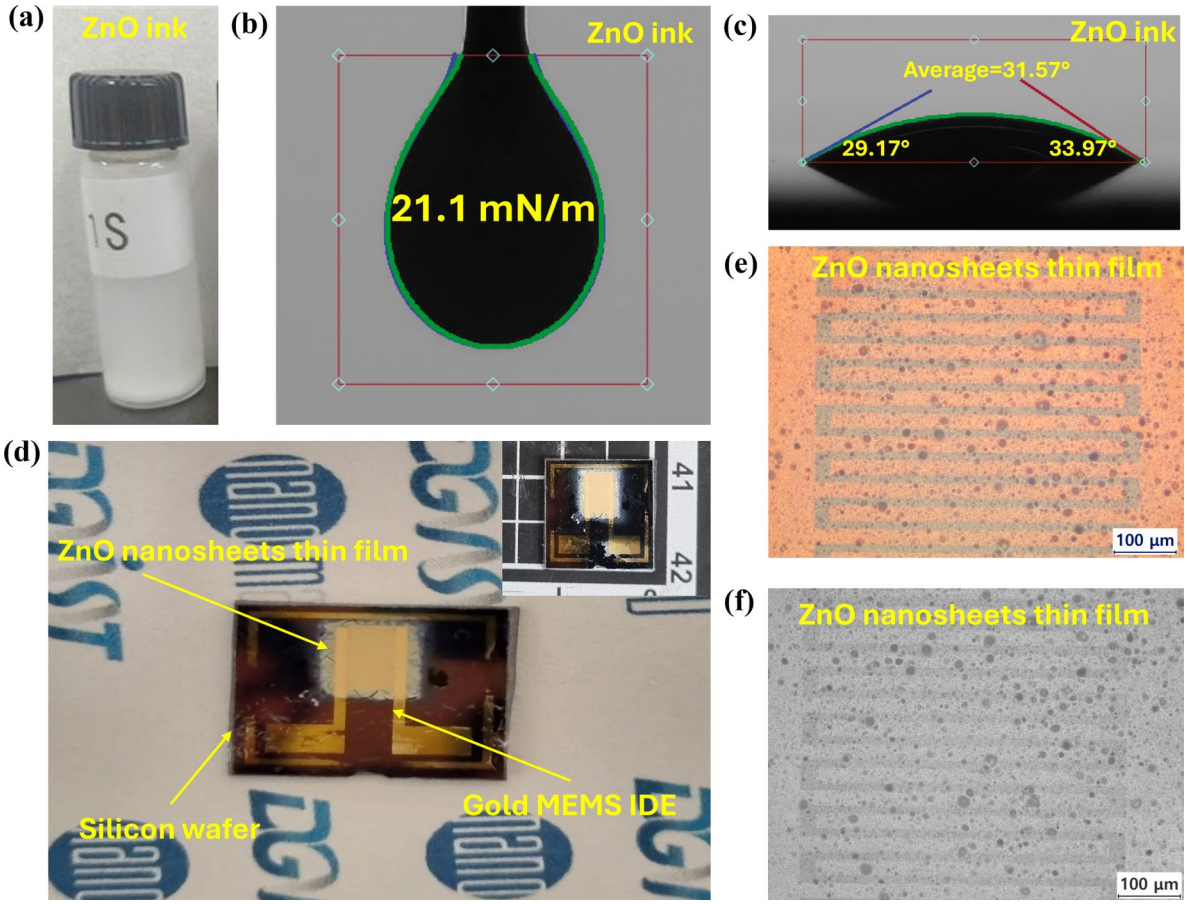

Fig. 3 ZnO ink and printed thin film: **a** Digital photo, **b** Surface tension, **c** Contact angle, **d** Digital photo of printed ZnO nanosheets on an oxidized silicon wafer, and **e**–**f** Optical microscope image of printed ZnO nanosheets

used to calculate gas sensor response (SR%) to baseline's resistance and response/recovery times. SR% was determined using Eq. 1 [25–29], providing a quantitative evaluation of the sensor's effectiveness in detecting NO_2 Eq. 2 [30].

$$SR\% = \frac{R_g - R_a}{R_a} * 100\% \quad n\text{-}type\ sensor\ Oxidizing\ gases \tag{1}$$

$$SR\% = \frac{I_a - I_g}{I_g} * 100\% \quad n\text{-}type\ sensor\ Oxidizing\ gases \tag{2}$$

Results and discussion

TEM analysis reveals that the ZnO is composed of nanosheet structures. This robust interaction plays a critical role in enhancing sensor performance, Fig. 2a. The ZnO nanosheets exhibit a uniform morphology with an average size of approximately 113 nm, as shown in Fig. 2b. Additionally, the ZnO displays sheet-like structures with sizes ranging from 50 to 250 nm, as illustrated in Fig. 2c.

XRD analysis shows the crystalline structure and phase composition of ZnO nanosheets, as shown in Fig. 2d. The XRD pattern revealed distinct peaks at 31.98°, 34.69°, 36.58°, 47.76°, 56.82°, 63.10°, 68.17°, and 69.35°, corresponding to the planes (100), (002), (101), (102), (110), (103), (112), and (201) respectively. These peaks align with the hexagonal wurtzite structure of ZnO (JCPDS No. 36-1451), confirming its crystalline nature [31].

XPS is a powerful tool for investigating the intricacies of a material electronic structure. XPS probes the electronic states of a solid by exciting electrons and measuring their kinetic energy. However, the interaction between the produced hole and mobile electrons can influence the resulting spectra, thus providing valuable information about the material's structure beyond its basic electronic states. Due to its potential for revealing detailed structural and electronic properties, XPS has been extensively used to study ZnO, particularly in

Table 2 Comparison table of NO_2 gas sensing performance of our work and reported works in literature

Materials	Fabrication Technique	NO_2 (ppm)	Temp (°C)	Response $SR_1 = (\Delta R/R_a) \times 100\%$ or $SR_2 = R_a/R_g$ or $SR_3 = R_g/R_a$	Response/Recovery time (s)	Reference
ZnO nanosheets	Spray printing/ photolithography	100	150	SR1 = 5298	96/600	This Work
ZnO nanosheets	Spray printing/ photolithography	100	RT	SR1 = 867	136.8/1723	This Work
ZnO Mesoporous sheets	Photolithography/spin coating	1	RT	SR1 = 130	180/150	[37]
ZnO-decorated MWCNTs	Spray printing	10	300	SR2 = 1.023	93.1/285.2	[38]
ZnO/CNTF-500	–	20	100	SR2 = 1.086	–/–	[39]
ZnO nanorods-ZnO:6	Dip-coating	100	175	SR1 = 580%	30/150	[29]
1 wt.%FMWCNT@ZnO	Sol–gel/spin coating	120	150	SR1 = 90	–/374	[40]
ZnO/m-SWCNTs	Spray Printing	15	RT	SR1 = 67.5	95/–	[41]
ZnO hierarchical nanostructure	Photolithograph/ physical vapor deposition	20	RT	SR3 = 32 SR3 = 2.5	72/69 in N_2 gas for recovery 1200/900 in air for recovery	[42]
MWCNT/ZnO film	CVD	25	60	SR1 = 10.5	–/–	[43]
SnO_2/graphene composite	Spray printing	5	150	SR3 = 72.6	129/107	[44]
ZnO@rGO	In-situ growth thin-film	10	RT	SR2 = 6.77	150/113	[45]
ZnO/Pd	Spin coating	1	RT/UV	SR1 = 1060	25/29	[46]
3D Graphene Nanotubes (GNT)@ZnO	–	50	RT/UV	SR1 = 47.5	300/200	[47]
ZnO nanorod/Au		1	RT	SR3 = 4.66	–/–	[48]
ZnO/SWCNTs (1:1)	Spray printing	5	RT	SR2 = 7	220/385	[49]

its nanophase form. In these nanostructures, XPS offers unique insights into how various dopants and defects modify electronic structures [32, 33]. The survey spectrum of ZnO (Fig. 2e) confirms the presence of zinc and oxygen as the primary elements, indicating minimal impurities.

The elemental composition of ZnO was quantified using EDX spectroscopy, Fig. 2f. The EDX spectra corresponding to pure ZnO were identified as zinc (Zn) and oxygen (O), with weight percentages of 76.25 and 23.75 wt.%, respectively. The elemental analysis and mapping revealed the visual distribution of elements of ZnO, which were crucial for improving their gas-sensing properties, Fig. 2g–i.

To formulate the ZnO ink, we used PVP as a binder to increase the stability of the ZnO film on the top of IDE, as discussed by Markos et al. [34]. Figure 3a–c shows the digital photo of our ZnO ink and its physical properties, such as surface tension and contact angle, which are 21.1 mN m^{-1} and 31.57°, respectively. Figure 3d–f presents the digital photo and optical microscope image of ZnO thin film. The ZnO sensor demonstrated exceptional sensor response towards NO_2 gas, primarily due to its high electron mobility and chemical stability compared to previously reported work, Table 2. However, the sensor response was substantially affected by both the operating temperature and the nature of the recovery gas [35]. In general, achieving adequate response and selectivity for NO_2 detection with pure ZnO requires high operating temperatures, typically around 300 °C as reported in the literature [3]. Figure 4a–f shows the raw data of the ZnO sensor in electrical current and resistance, which were used to calculate the SR%. The normalized data of the ZnO nanosheet sensor have been shown in Fig. 5a–f in electrical current and resistance which indicated the high performance of our sensor towards different concentrations of NO_2 gas. In our work, the gas sensor's performance test was conducted across three different temperatures of 25, 100, and 150 °C with varying NO_2 concentrations (20, 40, 60, 80, and 100 ppm), and the response was calculated from current according to Eq. 2 [30]. At these temperatures, the adsorption and desorption of NO_2 on the ZnO surface are enhanced, improving the efficiency. The minimum detectable gas concentration is a key indicator of a gas sensor's performance. The limit of detection (LOD) is calculated using the *LOD (ppm)=(3*rms)/slope*, where "rms" represents the root-mean-square value of the baseline signal noise. As shown in Fig. 6a, the full response of ZnO sensor to varying NO_2

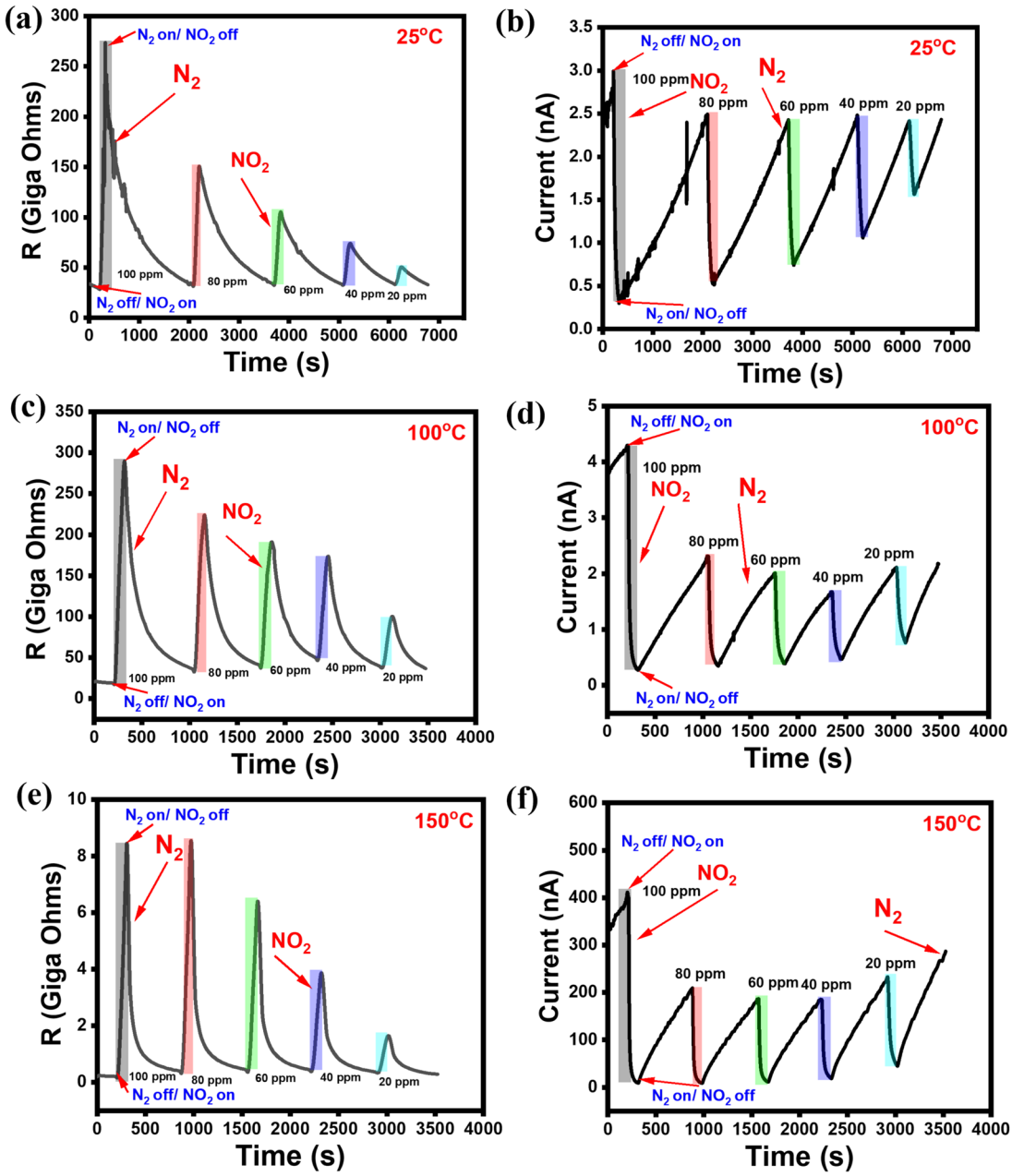

Fig. 4 Electrical resistance and current response of ZnO gas detection towards NO_2 gas at 80 V in Bias: **a**–**b** 25, **c**–**d** 100, and **e**–**f** 150 °C

gas concentrations was evaluated. Linear fitting analysis of the response yielded a slope value of 3.6, 4.22, and 25.2 at 25, 100, and 150 °C, respectively. Based on this, the LOD was determined to be 107, 68, and 1 part per billion (ppb), highlighting the capability of the sensor to detect NO_2 gas in different temperatures and concentrations in ppb and ppm ranges. Hence, what we noticed is that when the temperature increases, the LOD reduces due to the thermal activation energy, and this can be clearly seen in the effect of increasing temperature on the fast response and recovery, Fig. 6b, c. Therefore, the ZnO sensor demonstrated its highest sensitivity of 867, 1333, and 5298% at a NO_2 concentration of 100 ppm with the operating temperatures of 25, 100, and 150 °C, respectively, as shown in Fig. 6a. The corresponding response and recovery times were 137/1742, 114/733, and 96/600 s at 100 ppm for 25, 100, and 150 °C, respectively, as illustrated in Fig. 6b, c. Figure 6d presents the selectivity towards 100 ppm of NO_2 with EtOH, isopropanol (IPA), methanol (MeOH), and acetone, which gives evidence of the high selectivity of the

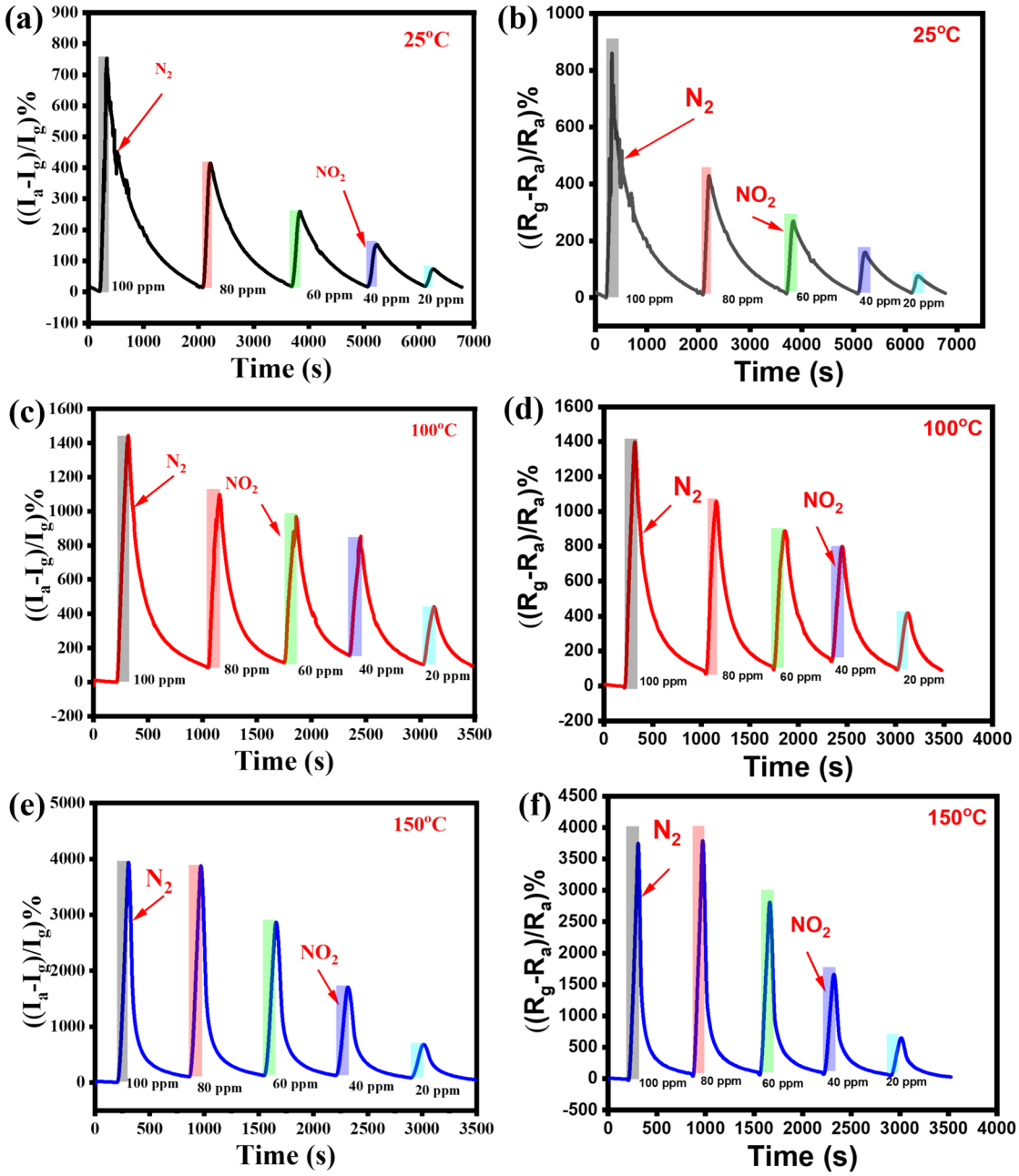

Fig. 5 The gas sensing performance of ZnO nanosheets sensor towards NO_2 gas: Normalized Current and resistance change percentage to baseline and gas at **a**–**b** 25, **c**–**d** 100, and **e**–**f** 150 °C at different concentrations of NO_2 (20, 40, 60, 80, and 100 ppm)

ZnO sensor toward NO_2 at RT. As discussed by Shan et al. [36], joule heating increases the performance of the ZnO towards NO_2 gas due to oxidation–reduction reaction at ZnO surface. Additionally, Fig. 6e highlights the consistent performance of the ZnO sensor across 10 cycles of exposure to 100 ppm NO_2 gas, which shows that the performance increases with increasing the number of cycles due to the activation of the ZnO surface by the introduction of NO_2 gas. Temperature-induced activation of the ZnO material, which enhanced its gas sensing and recovery performance, was responsible for the variation in response and recovery times. Figure 6f explains the reaction mechanism of ZnO with NO_2 gas. Upon exposure to NO_2 gas, the ZnO surface efficiently adsorbs the gas at its active sites, allowing it to capture electrons from the ZnO surface. This process is described by Eqs. 3, 4, and 5 [27], underscoring the

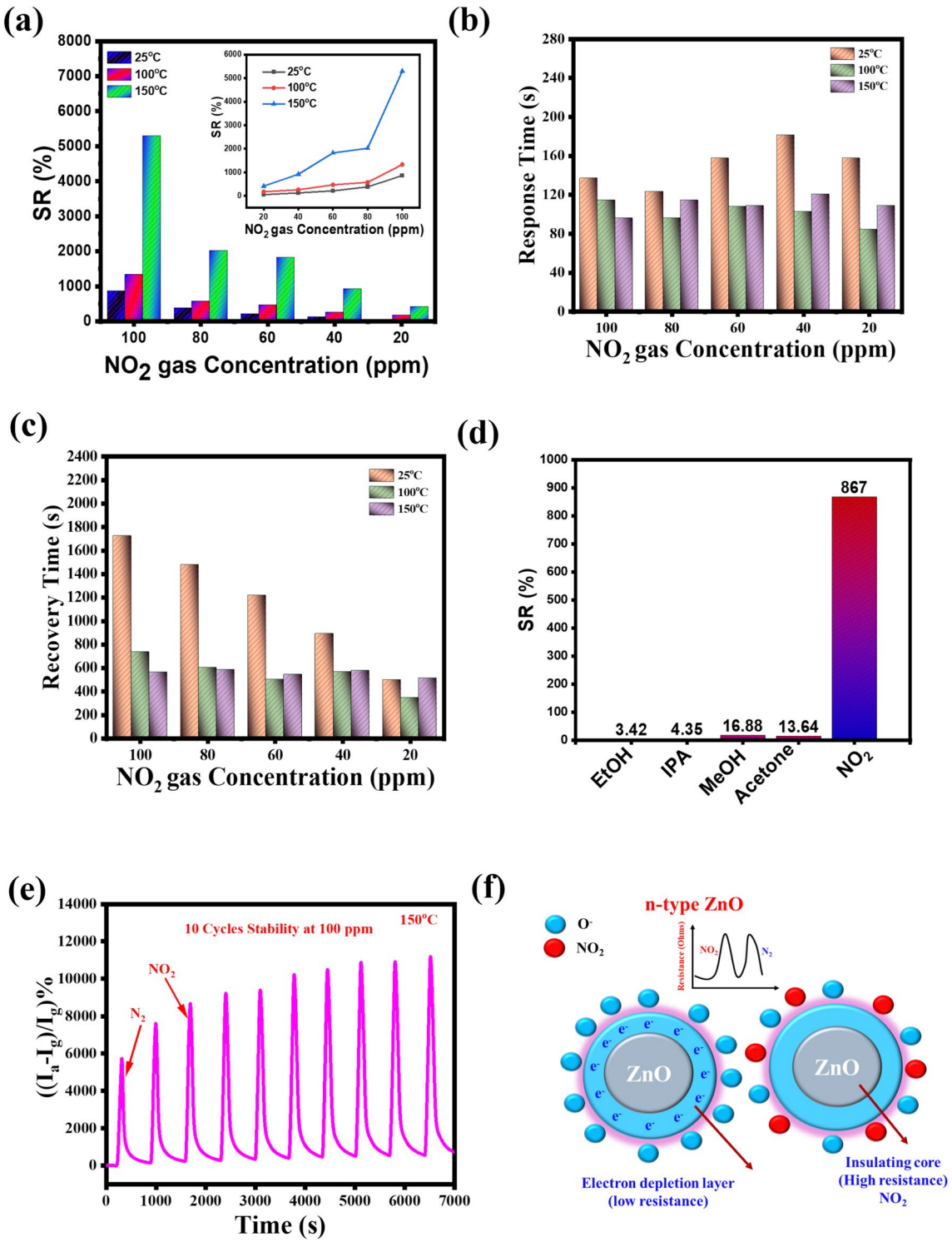

Fig. 6 Gas sensing performance of sensitivity, recovery and response times, selectivity, stability testing, and sensing mechanism: **a** Sensitivity at different concentrations of NO_2 gas (20, 40, 60, 80, and 100 ppm) at 25, 100, and 150 °C, **b**–**c** Response and recovery times at different NO_2 gas concentrations, **d** Selectivity of NO_2 gas sensor towards EtOH, IPA, MeOH, and Acetone at RT, **e** Gas sensing stability at 100 ppm and 150 °C for 10 cycles, and **f** Schematic illustration of gas sensing mechanism towards NO_2 gas

high efficiency and response of the sensor. ZnO nanosheets demonstrate exceptional potential as NO_2 sensors, offering enhanced performance and operational efficiency for real-time monitoring.

$$NO_{x(gas)} + e^- \rightarrow NO^-_{X(ads.)} \quad (3)$$

$$NO_{x(gas)} + O^-_{(ads.)} + 2e^- \rightarrow NO^-_{X(ads.)} + 2O^-_{(ads.)} \quad (4)$$

$$NO_{x(gas)} + O^-_{(ads.)} + 2e^- \rightarrow NO^-_{X(ads.)} + 2O^{2-}_{(ads.)} \quad (5)$$

Conclusions

This study extensively evaluated a NO_2 gas sensor based on ZnO nanosheets using a range of analytical techniques, including TEM, SEM, EDX, XRD, XPS, and gas sensing performance. ZnO demonstrated high sensor response towards NO_2 gas due to its excellent electron mobility and chemical stability. However, achieving optimal performance typically requires high operating temperatures, which limited its practicality. By utilizing ZnO nanosheets, the sensor achieved enhanced response, fast response and recovery times, and efficient operation. XRD analysis confirmed the crystalline structure of the ZnO nanosheets and their successful functionalization, while EDX mapping verified the uniform distribution of elemental components. The gas sensing performance of the ZnO nanosheets was particularly noteworthy, with a sensitivity of 5298% and response/recovery times of (96/600 s) at 150 °C and 100 ppm NO_2. These results highlight the potential of ZnO nanosheets as a highly effective NO_2 sensor, addressing the critical need for real-time monitoring with improved performance and operational efficiency.

Acknowledgements
This work is supported by the National Research Foundation of Korea (NRF) (RS-2024-00431411, RS-2024-00346135), which is funded by the Ministry of Science and ICT, Korea.

Author contributions
Mohamed Ahmed BELAL: Conceptualization, Writing-Original Draft, Sugato HAJRA: Writing- Editing, Visualization, Swati PANDA: Writing- Editing, Visualization, Kushal Ruthvik KAJA: Writing- Editing, Visualization, Kyeong Jun PARK: Visualization, Hoe Joon KIM: Supervision, Funding Acquisition, Writing-Editing.

Data availability
No datasets were generated or analysed during the current study.

Declarations

Competing interests
The authors declare no competing interests.

Author details
[1]Department of Robotics Engineering, Daegu Gyeongbuk Institute of Science and Technology (DGIST), Daegu 42988, Korea.

Received: 15 December 2024 Accepted: 21 May 2025
Published online: 06 June 2025

References

1. N.A.Q.M. Network
2. A.L. Association
3. Belal M, Hajra S, Panda S, Kaja KR, Abdo MMM, Abd El-Moneim AAE-M, Janas D, Mishra YK, Kim HJ (2025) J Mater Chem A
4. Barthwal S, Singh B, Singh NB (2018) ZnO-SWCNT nanocomposite as NO_2 gas sensor. Mater Today-Proc 5:15439–15444
5. Bhangare B, Ramgir NS, Jagtap S, Debnath AK, Muthe KP, Terashima C, Aswal DK, Gosavi SW, Fujishima A (2019) XPS and Kelvin probe studies of SnO_2/RGO nanohybrids based NO_2 sensors. Appl Surf Sci 487:918–929
6. Lee K, Hajra S, Sahu M, Kim HJ (2021) Colossal dielectric response, multiferroic properties, and gas sensing characteristics of the rare earth orthoferrite $LaFeO_3$ ceramics. J Alloys Compounds 882:160634
7. Lee K, Sahu M, Hajra S, Mohanta K, Kim HJ (2021) Effect of sintering temperature on the electrical and gas sensing properties of tin oxide powders. Ceram Int 47:22794–22800
8. Nasser AH, Guo L, ELnaggar H, Wang Y, Guo X, AbdelMoneim A, Tsubaki N (2018) Mn–Fe nanoparticles on a reduced graphene oxide catalyst for enhanced olefin production from syngas in a slurry reactor. RSC Adv 8:14854–14863
9. Bu X, Ding K, Wu Q, Yuan Y, Liu W, Han C, Wang X, Li X (2023) The synthesis of metal organic frameworks derived 3D porous V_2O_5 microrods for NO_2 detection and its UV-enhanced sensing performance. Sensor Actuat B Chem 393:134321
10. Chen GL, Lv MS, Sui LL, Deng ZP, Xu YM, Huo LH, Gao S (2023) Low-temperature and dual-sensing NO_2/dimethylamine sensor based on single-crystal WO3 nanoparticles-supported sheets synthesized by simple pyrolysis of spoiled WCl6 powder. Chem Eng J 464:142528
11. Zhang C, Luo Y, Xu J, Debliquy M (2019) Room temperature conductive type metal oxide semiconductor gas sensors for NO_2 detection. Sensor Actuat A Phys 289:118–133
12. Lee K, Hajra S, Sahu M, Mishra YK, Kim HJ (2022) Co^{+3} substituted gadolinium nano-orthoferrites for environmental monitoring: synthesis, device fabrication, and detailed gas sensing performance. J Ind Eng Chem 106:512–519
13. Belal MA, Yousry R, Taulo G, AbdelHamid AA, Rashed AE, El-Moneim AA (2023) Layer-by-layer inkjet-printed manganese oxide nanosheets on graphene for high-performance flexible supercapacitors. ACS Appl Mater Interfaces 15:53632–53643
14. Bayoumy AM, Hessein A, Ahmed Belal M, Ezzat M, Ibrahim MA, Osman A, Abd El-Moneim A (2024) Microdrop InkJet printed supercapacitors of graphene/graphene oxide ink for flexible electronics. J Power Sour 617:235145
15. Belal MA, Khalil HH, Mahajan RL, Rashed AE, Khattab SN, El-Moneim AA (2024) Layered structure design of inkjet-printed graphene/Co_3O_4 for high-performance flexible microsupercapacitors. J Energy Storage 101:113900
16. Peřinka N, Držková M, Randjelović DV, Bondavalli P, Hajná M, Bober P, Syrový T, Bonnassieaux Y, Stejskal J (2014) Characterization of polyaniline-based ammonia gas sensors prepared by means of spray coating and ink-jet printing. Sens Lett 12:1620–1627
17. Zhou C, Shi N, Jiang X, Chen M, Jiang J, Zheng Y, Wu W, Cui D, Haick H, Tang N (2022) Techniques for wearable gas sensors fabrication. Sensor Actuat B Chem 353:131133
18. Vasquez S, Angeli MAC, Petrelli M, Ahmad M, Shkodra B, Salonikidou B, Sporea RA, Rivadeneyra A, Lugli P, Petti L (2023) Comparison of printing techniques for the fabrication of flexible carbon nanotube-based ammonia chemiresistive gas sensors. Flex Print Electron 8:035012
19. Taulo GT, Shaalan NM, Mohamed GG, Ayad MM, El-Moneim AA (2024) Inkjet printing of SnO_2 nanoparticles with exposed high-energy facets for CO gas sensing. Ceram Int 50:18638–18646
20. Tang Y, Lai P, Hu Z, Luo Y, Wang H, Yu L (2023) A hard mask process and alignment device aims to achieve high consistency and mass-scale production of gas sensors based on spraying hydrothermal gas sensing material. Rev Sci Instrum 94

21. Abdelhalim A, Falco A, Loghin F, Lugli P, Salmerón JF, Rivadeneyra A (2016) 2016 IEEE SENSORS, IEEE, pp 1–3
22. Peřinka N, Držková M, Randjelović DV, Bondavalli P, Hajná M, Bober P, Syrový T, Bonnassieaux Y, Stejskal J (2015) Application of Ink-Jet printing and spray coating for the fabrication of polyaniline/poly(N-Vinylpyrrolidone)-based ammonia gas sensor. Key Eng Mater 644:61–64
23. Lee G, Sim JH, Oh G, Won M, Mantry SP, Kim DS (2023) Electrostatic spray deposition of al-doped ZnO thin films for acetone gas detection. Processes 11:3390
24. Anbalagan S, Manojkumar K, Muthuramalingam M, Hajra S, Panda S, Sahu R, Joon Kim H, Sundaramoorthy A, Nithyavathy N, Vivekananthan V (2024) Progress and recent advances in self-powered gas sensing based on triboelectric and piezoelectric nanogenerators. Chem Eng J 497:154740
25. Park JY, Kwak Y, Lim HR, Park SW, Lim MS, Cho HB, Myung NV, Choa YH (2022) Low-temperature highly selective and sensitive NO_2 gas sensors using CdTe-functionalized ZnO filled porous Si hybrid hierarchical nanostructured thin films. J Hazard Mater 438:129412
26. Jaiswal J, Singh P, Chandra R (2021) Low-temperature highly selective and sensitive NO_2 gas sensors using CdTe-functionalized ZnO filled porous Si hybrid hierarchical nanostructured thin films. Sensor Actuat B Chem 327:128862
27. Birajdar SN, Adhyapak PV (2020) Palladium-decorated vanadium pentoxide as NOx gas sensor. Ceram Int 46:27381–27393
28. Me DM, Sundaram NG, Singh A, Singh AK, Kalidindi SB (2019) An amine functionalized zirconium metal–organic framework as an effective chemiresistive sensor for acidic gases. Chem Commun 55:349–352
29. Vanalakar SA, Patil VL, Harale NS, Vhanalakar SA, Gang MG, Kim JY, Patil PS, Kim JH (2015) Controlled growth of ZnO nanorod arrays via wet chemical route for NO_2 gas sensor applications. Sensor Actuat B Chem 221:1195–1201
30. Zampiceni E, Bontempi E, Sberveglieri G, Depero LE (2002) Mixed oxides Sn02-Mo0x thin felms for selective gas sensing, sensors and microsystems. World Scientific, pp 115–123
31. Narayanan N, Kannoth DN (2016) Exploring p type conductivity in ZnO thin films by In–N codoping for homo-junction devices. J Mater Sci Mater Electron 28:5962–5970
32. Pandey SK, Pandey SK, Mukherjee C, Mishra P, Gupta M, Barman SR, D'Souza SW, Mukherjee S (2013) Effect of growth temperature on structural, electrical and optical properties of dual ion beam sputtered ZnO thin films. J Mater Sci Mater Electron 24:2541–2547
33. Sahai A, Goswami N (2014) Probing the dominance of interstitial oxygen defects in ZnO nanoparticles through structural and optical characterizations. Ceram Int 40:14569–14578
34. Ezzat M, Rashed AE, Sabra SA, Haroun M, Abd El-Moneim A (2023) Fully inkjet-printed graphene/gold nonenzymatic biosensor for glucose detection. Mater Today Commun 37:107549
35. Cho B, Kim AR, Park Y, Yoon J, Lee YJ, Lee S, Yoo TJ, Kang CG, Lee BH, Ko HC, Kim DH, Hahm MG (2015) Bifunctional sensing characteristics of chemical vapor deposition synthesized atomic-layered MoS_2. ACS Appl Mater Interfaces 7:2952–2959
36. Fan S-W, Srivastava AK, Dravid VP (2010) Nanopatterned polycrystalline ZnO for room temperature gas sensing. Sensor Actuat B Chem 144:159–163
37. Chen R, Wang J, Xiang L (2018) Facile synthesis of mesoporous ZnO sheets assembled by small nanoparticles for enhanced NO_2 sensing performance at room temperature. Sensor Actuat B Chem 270:207–215
38. Kwon YJ, Mirzaei A, Kang SY, Choi MS, Bang JH, Kim SS, Kim HW (2017) Synthesis, characterization and gas sensing properties of ZnO-decorated MWCNTs. Appl Surf Sci 413:242–252
39. Woo S, Jo M, Lee J-S, Choi S-H, Lee S, Jeong HS, Choi S-J (2021) Metal-organic frameworks-driven ZnO-functionalized carbon nanotube fiber for NO_2 sensor. J Sens Sci Technol 30:369–375
40. Gholami P, Rashidi A, Khaleghi Abbasabadi M, Pourkhalil M, Jahangiri M, Izadi N (2020) Synthesis and characterization of ZnO-functionalized multiwall carbon nanotubes nanocomposite as NOx gas sensor. Res Chem Intermed 46:3911–3927
41. Li X, Wang J, Xie D, Xu J, Xia Y, Xiang L (2017) Enhanced p-type NO_2-sensing properties of ZnO nanowires utilizing CNTs electrode. Mater Lett 206:18–21
42. Pan X, Zhao X, Chen J, Bermak A, Fan Z (2015) A fast-response/recovery ZnO hierarchical nanostructure based gas sensor with ultra-high room-temperature output response. Sensor Actuat B Chem 206:764–771
43. Kim H-S, Jang K-U (2018) The detection characterization of NOX gas using the MWCNT/ZnO composite film gas sensors by heat treatment. J Korean Inst Electr Electr Mater Eng 31:521–526
44. Kim HW, Na HG, Kwon YJ, Kang SY, Choi MS, Bang JH, Wu P, Kim SS (2017) Microwave-assisted synthesis of graphene–SnO_2 nanocomposites and their applications in gas sensors. ACS Appl Mater Interfaces 9:31667–31682
45. Gao R, Gao L, Zhang X, Gao S, Xu Y, Cheng X, Guo G, Ye Q, Zhou X, Major Z, Huo L (2021) The controllable assembly of the heterojunction interface of the ZnO@rGO for enhancing the sensing performance of NO_2 at room temperature and sensing mechanism. Sensor Actuat B Chem 342:130073
46. Wang J, Hu C, Xia Y, Komarneni S (2020) Highly sensitive, fast and reversible NO_2 sensors at room-temperature utilizing nonplasmonic electrons of ZnO/Pd hybrids. Ceram Int 46:8462–8468
47. Dong L, Wang Y, Wu Z, Liu W, Ying S, Huang M, Peng C (2020) Gas sensing properties of 3D graphene nanotubes (GNT)@ZnO at room temperature. IOP Conf Ser Earth Environ Sci 446:022032
48. Wang J, Fan S, Xia Y, Yang C, Komarneni S (2020) Room-temperature gas sensors based on ZnO nanorod/Au hybrids: visible-light-modulated dual selectivity to NO_2 and NH_3. J Hazard Mater 381:120919
49. Park S, Byoun Y, Kang H, Song YJ, Choi SW (2019) ZnO nanocluster-functionalized single-walled carbon nanotubes synthesized by microwave irradiation for highly sensitive NO_2 detection at room temperature. ACS Omega 4:10677–10686

Publisher's Note